nature chemical biology

© 2005 Nature Publishing Group http://www.nature.com/naturechemicalbiology

Dynamic imaging of protease activity with fluorescently quenched activity-based probes

Galia Blum[1], Stefanie R Mullins[2,3], Kinneret Keren[4], Marko Fonovič[1,5], Christopher Jedeszko[2], Mark J Rice[1], Bonnie F Sloane[2,3] & Matthew Bogyo[1]

Protease activity is tightly regulated in both normal and disease conditions. However, it is often difficult to monitor the dynamic nature of this regulation in the context of a live cell or whole organism. To address this limitation, we developed a series of quenched activity-based probes (qABPs) that become fluorescent upon activity-dependent covalent modification of a protease target. These reagents freely penetrate cells and allow direct imaging of protease activity in living cells. Targeted proteases are directly identified and monitored biochemically by virtue of the resulting covalent tag, thereby allowing unambiguous assignment of protease activities observed in imaging studies. We report here the design and synthesis of a selective, cell-permeable qABP for the study of papain-family cysteine proteases. This probe is used to monitor real-time protease activity in live human cells with fluorescence microscopy techniques as well as standard biochemical methods.

Proteases play fundamental roles in the control of both normal and disease processes. Alterations in protease expression and activity patterns underlie many human pathological processes, including cancer, arthritis, osteoporosis, atherosclerosis and neurodegenerative disorders[1]. Thus, a detailed understanding of how, when and where a particular protease functions in a complex cellular environment is required to better understand its role in the promotion of disease. Perhaps the most powerful way to address these issues is to develop methods that allow dynamic imaging of protease activity within a living cell or organism.

Recently, a number of elegant methods have been developed to image enzymatic activities using both invasive and whole-body imaging methods (for review, see ref. 2). Virtually all of these methods make use of reporter substrates that, when processed by a given enzyme target, produce a signal that can be visualized with common imaging modalities. Although these methods have clearly paved the way for the application of activity-based reporters to diagnostic medicine, they suffer from several features, such as lack of specificity and cell permeability, as well as rapid diffusion, that may limit their use in high-resolution studies of enzyme regulation and localization.

Activity-based probes (ABPs) are small molecules that modify a defined set of enzyme targets on the basis of their ability to form specific covalent bonds with key catalytic residues (for reviews, see refs. 3–7). Because this labeling reaction is mechanism based and requires enzyme activity, the extent of probe modification serves as an indirect readout of activity levels within a given sample. Probes can be designed to target a number of different classes of enzymes through optimization of both reactive functional groups and the scaffolds used to carry the reporter tag. In the past five years, a number of new classes of ABPs have been developed and used to dissect the function of various enzyme families (see reviews, refs. 3–7). The most

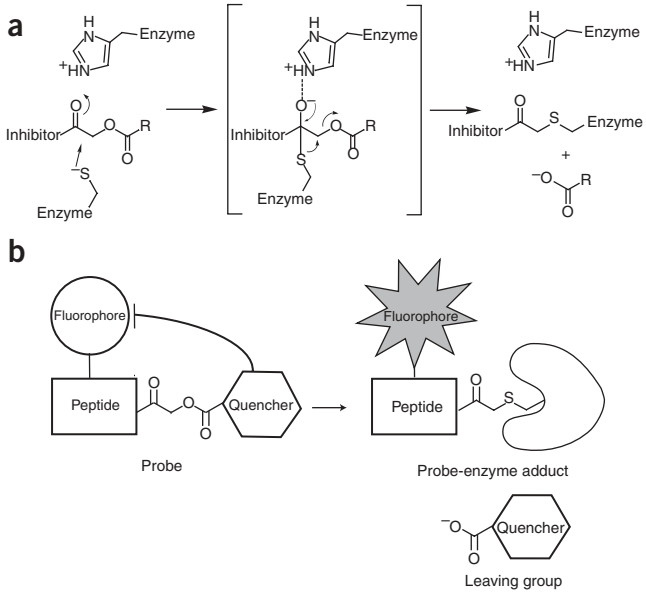

Figure 1 Design of a qABP. (**a**) Mechanism of covalent inhibition of a cysteine protease by an acyloxymethyl ketone. (**b**) Activity-dependent labeling of a cysteine protease target by a qABP. Covalent modification of the target results in loss of the quenching group, resulting in production of a fluorescently labeled enzyme.

[1]Departments of Pathology, [4]Biochemistry and [6]Microbiology and Immunology, Stanford University School of Medicine, 300 Pasteur Dr., Stanford, California 94305, USA. [2]Department of Pharmacology and [3]Barbara Ann Karmanos Cancer Institute, Wayne State University School of Medicine, 540 East Canfield, Detroit, Michigan 48201, USA. [5]Department of Biochemistry and Molecular Biology, Jozef Stefan Institute, Jamova 39, 1000 Ljubljana, Slovenia. Correspondence and requests for materials should be addressed to M.B. (mbogyo@stanford.edu).

Published online 14 August 2005; doi:10.1038/nchembio728

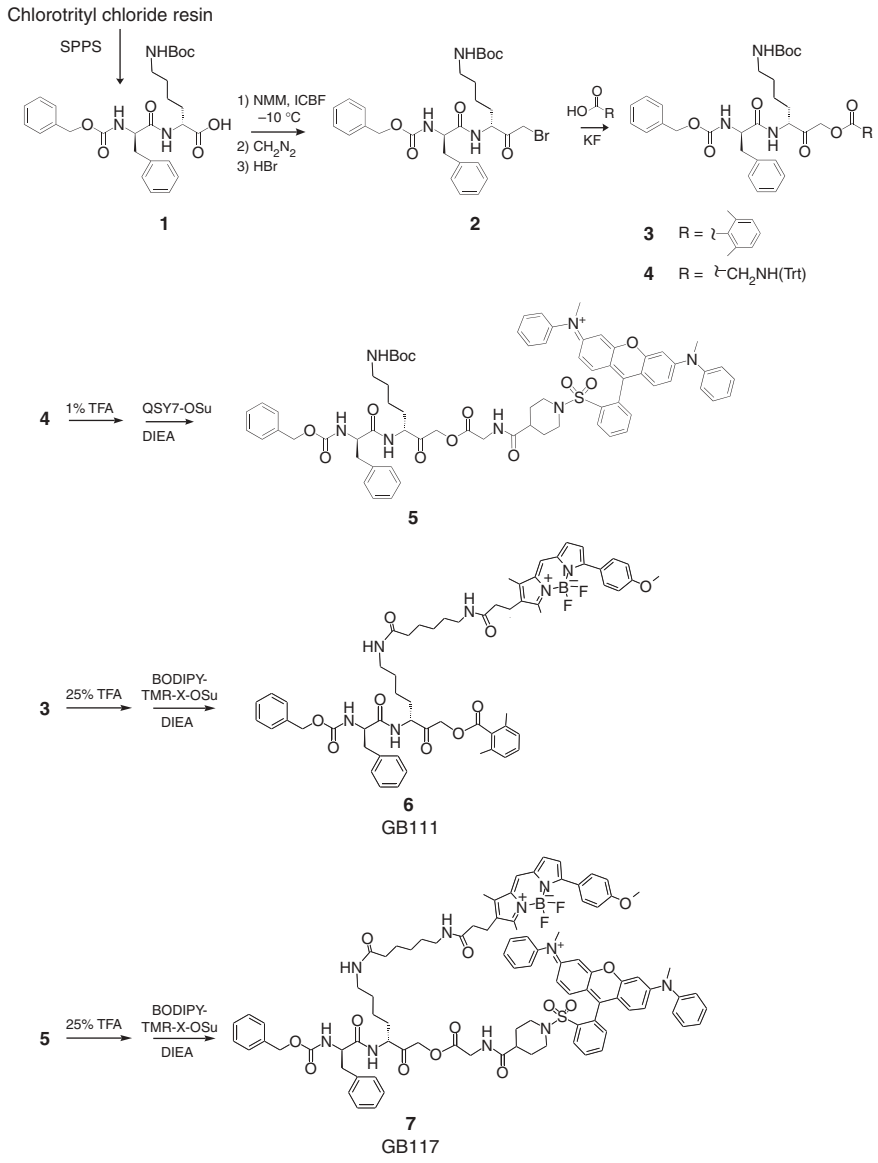

Scheme 1 Synthesis of the qABP GB117 and the corresponding control ABP GB111. The fully protected dipeptide (**1**) was synthesized on solid support with standard solid-phase peptide synthesis (SPPS) and was converted to the corresponding BMK (**2**) in solution. The resulting BMK was converted to the 2,6-dimethyl benzoic acid AOMK (**3**) or the *N*-trityl-protected glycine AOMK (**4**). Selective removal of the *N*-trityl group from (**4**) followed by coupling of the QSY7 quencher yielded AOMK intermediate (**5**). Finally, removal of the Boc-protecting group on lysine of (**3**) and (**5**) followed by coupling of the BODIPY-TMR-X yielded the final products GB111 and GB117. NMM, *N*-methyl morpholine; IBCF, isobutylchloroformate; HBr, hydrogen bromide; TFA, trifluoroacetic acid; DIEA, diisopropylethylamine.

© 2005 Nature Publishing Group http://www.nature.com/naturechemicalbiology

well-established and heavily used probes are those that target proteolytic enzymes[8–19]. ABPs that target serine and cysteine proteases have been applied to studies of protease function in processes such as parasite invasion[20], prohormone processing[21], transcriptional regulation[22], cataract formation[23], natural killer cell function[24] and cancer progression[25–27].

A number of ABPs carrying a range of fluorescent reporters have also been described[8,12,15,27,28]. The fluorescent group serves as a highly sensitive tag that enables visualization of labeled targets after their biochemical separation. Fluorescently labeled ABPs have also been used to directly image enzyme activity with microscopy techniques. We recently demonstrated that a fluorescent ABP can be used in a mouse model for pancreatic cancer to image cysteine protease activity during multiple stages of tumor formation[27]. The use of ABPs for imaging applications has the major advantage of the formation of a permanent covalent bond with the enzyme, thus allowing direct biochemical analysis of targets. However, the major limitation of these probes is their general fluorescence both when bound to an enzyme target and when free in solution. To overcome this limitation, we set out to design quenched probes (qABPs) that become fluorescent only after covalent modification of a protease target.

We initially chose to focus on the acyloxymethyl ketone (AOMK) reactive group for probe design, as this 'warhead' targets diverse families of cysteine proteases[9,29]. More importantly, the mechanism of covalent modification of a cysteine protease by an AOMK involves the loss of its acyloxy group[29] (**Fig. 1a**). Thus, a probe carrying a fluorescent reporter group on its peptide scaffold and a highly efficient quenching molecule attached to the acyloxy leaving group should result in a quenched probe that only becomes fluorescent upon covalent labeling of an enzyme target (**Fig. 1b**). We initially focused our efforts on probes that target the papain family of cysteine proteases, as this family has been extensively studied with ABPs and a number of cell-permeable reagents have successfully been designed[9,11,14,15]. Our first generation of qABPs made use of the fluorescein/4-([4-(dimethylamino)phenyl]azo) benzoic acid (DABCYL) pair, which was shown to be effective for related applications[30,31]. Unfortunately, we found that although it was possible to use cell-permeable BODIPY analogs of fluorescein, the DABCYL group prevented probes from freely entering cells (data not shown). Furthermore, we found that direct attachment of the DABCYL quenching group to the reactive hydroxy ketone methylene resulted in probes that were highly unstable in aqueous solution and also showed markedly reduced potency for target proteases, presumably because of the proximity of the bulky quencher to the active site (data not shown). We therefore shifted our attention to the larger but potentially more cell-permeable quenching group QSY7 and attached this group to the probe through a linker to improve stability and potency.

We carried out the synthesis of the resulting quenched probe GB117 and its corresponding nonquenched control GB111 using a combination of solid and solution-phase chemistries (**Scheme 1**). This synthetic route was chosen over recently reported solid-phase methods[9] because of the formation of an intramolecular acyl transfer reaction on resin that was observed when an aliphatic acyloxy group was used in place of the 2,6-dimethyl benzoyl group (G.B. and M.B., unpublished data). The fully protected carbobenzoxy-capped phenylalanine-lysine

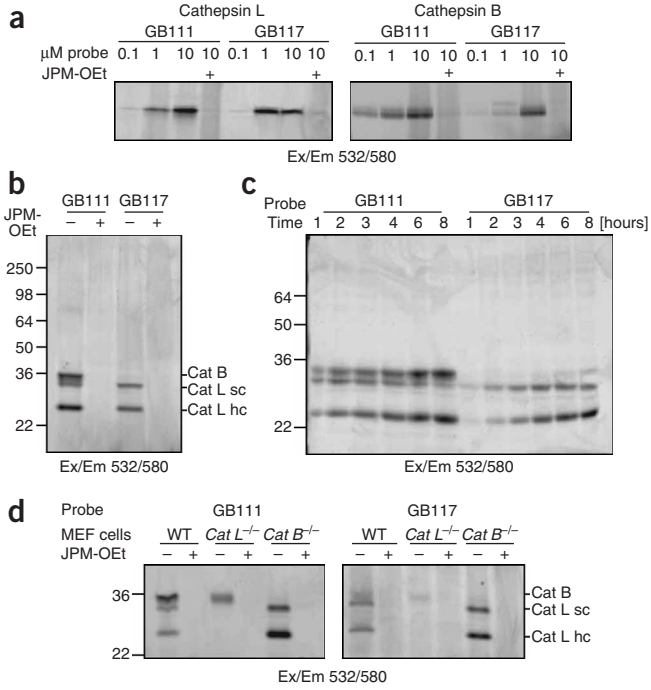

Figure 2 Labeling of recombinant cathepsins and intact cells with the control ABP and qABP. (**a**) Labeling of purified recombinant cathepsin B and L with the control ABP GB111 and the qABP GB117. Recombinant enzymes in buffer (pH 5.5) were either treated with the general papain-family inhibitor JPM-OEt (50 μM; +) or with DMSO (0.1%; –) for 30 min followed by labeling with probes at the indicated concentrations for 30 min. Samples were analyzed by SDS-PAGE and fluorescent signal was measured by scanning of gels with a Typhoon laser flatbed scanner. (**b**) Intact monolayers of NIH-3T3 cells were pretreated either with the general papain-family protease inhibitor JPM-OEt (50 μM) or with control DMSO (0.1%) for 1 h and labeled by addition of GB111 and GB117 (1 μM) to culture medium for 3 h. Crude detergent lysates were normalized for total protein, separated by SDS-PAGE, and visualized by scanning of the gel with a Typhoon flatbed laser scanner. (**c**) Monolayers of NIH-3T3 cells were labeled by addition of GB111 or GB117 (1 μM) to cultured medium for a series of times as indicated. Labeled proteases were analyzed as in **b**. (**d**) Labeling of cathepsin targets in fibroblasts derived from WT, *Cat B*$^{-/-}$ and *Cat L*$^{-/-}$ mice. Intact fibroblasts were pretreated with JPM-OEt (50 μM) or DMSO (0.1%) for 1 h and then labeled with 1 μM of either the control ABP GB111 (left) or the qABP GB117 (right). Cells were collected, lysed and analyzed after SDS-PAGE as in **b** and **c**. Cat L sc, cathepsin L single-chain form. Cat L hc, cathepsin L heavy-chain form.

dipeptide (**1**) was synthesized with standard solid-phase peptide synthesis and was converted to the corresponding bromo-methyl ketone (BMK, **2**) in solution. Coupling of 2,6-dimethyl benzoic acid with the BMK resulted in the AOMK intermediate (**3**) for use in the synthesis of the nonquenched control. Conversion of the BMK via *N*-trityl-protected glycine yielded the AOMK (**4**) that was coupled to the commercially available QSY7 quenching group after removal of the trityl group to produce intermediate (**5**). Finally, removal of the *t*-butoxy carbonyl (Boc) protecting group on the side chain of lysine in intermediates (**3**) and (**5**) allowed attachment of the BODIPY-TMR-X fluorophore to produce the desired ABP GB111 (**6**) and qABP GB117 (**7**).

We attached the fluorophore to the probe at the P1 lysine side chain to optimize proximity to the quenching group. Previous work has shown that the majority of critical substrate interactions take place in the P2 position of the papain-family proteases[32]. This close positioning resulted in a probe that showed greater than 70-fold quenching when compared with the nonquenched control probe (**Supplementary Fig. 1** online). This amount of quenching is sufficient for imaging applications and is in line with other reported proximity-induced quenching reagents[30]. We also found that the fluorophore could be attached to more distal positions (that is, P2, P3 or the amino terminus) while retaining sufficient quenching for imaging applications (data not shown). When we performed kinetic inhibition studies for the two papain-family proteases, cathepsins B and L, we found that modification of the P1 lysine of the free amine intermediate of GB111 (NH2-GB111) resulted in a 100-fold loss of potency toward cathepsin L and a 30-fold loss of potency for cathepsin B (**Supplementary Table 1** online). Nonetheless, the resulting fluorescent probes retained substantial activity that was deemed sufficient to obtain efficient labeling of targets. Interestingly, replacement of the 2,6-dimethyl benzoyl group on GB111 with the bulky QSY7 quencher resulted in a larger drop in potency of the probe toward cathepsin B than toward cathepsin L (**Supplementary Table 1**). This result can most likely be explained by the so-called occluding loop of cathepsin B blocking access of extended peptides into the prime side-binding sites[33]. Modeling of the two probes into the high-resolution structures of cathepsins B and L confirmed that the QSY7 group potentially produces van der Waals clashes with the occluding loop of cathepsin B (**Supplementary Fig. 2** online).

We next examined if GB111 and GB117 were capable of forming stable covalent linkages to cathepsin targets. Labeling of purified recombinant cathepsin B and L confirmed the kinetic results and demonstrated that both probes label the recombinant enzyme in solution, resulting in an SDS-stable covalent linkage (**Fig. 2a**). This labeling could also be specifically competed by pretreatment of the enzymes with the broad-spectrum papain-family cysteine protease inhibitor JPM-OEt[27]. Furthermore, the same drop in potency of GB117 toward cathepsin B was observed in the *in vitro* labeling profiles, thus confirming the relative selectivity of GB117 for cathepsin L. However, we did observe labeling of additional purified cathepsin targets (cathepsins X and S; data not shown) by both GB111 and GB117 suggesting that these probes may label multiple targets in cell types with high expression of cathepsins other than cathepsins B and L.

Having confirmed that both the qABP and the control probe label multiple papain-family proteases *in vitro* at reasonable kinetic rates, we set out to determine whether these probes could label endogenous enzyme targets in intact cells. The probes were added to monolayers of live NIH-3T3 cells; this step was followed by collection, lysis of cells and analysis by SDS-PAGE (**Fig. 2b**). These initial results confirmed that both probes freely penetrated cells and labeled a series of protease targets in a highly selective way. Furthermore, the probes showed virtually no background labeling when papain-family proteases were inactivated by pretreatment of cells with JPM-OEt. Kinetic analysis of the labeling of the protease targets indicated that GB117 had a slower rate of modification than did GB111, suggesting that extended labeling times would be required to obtain optimal signal (**Fig. 2c**). Interestingly, the pattern of proteases labeled by GB111 included a species around 33 kDa that was only faintly labeled by GB117 at extended time points. We predicted that this species might be cathepsin B on the basis of its size and our findings that suggested that GB117 has reduced potency toward this target (**Supplementary Table 1** and **Fig. 2a**). To confirm the identity of the labeled species, we performed similar experiments in intact fibroblast cells derived from wild type (WT) and cathepsin B– and cathepsin L–knockout mice (*Cat B*$^{-/-}$ and *Cat L*$^{-/-}$, respectively; **Fig. 2d**). As expected, the 33-kDa species

© 2005 Nature Publishing Group http://www.nature.com/naturechemicalbiology

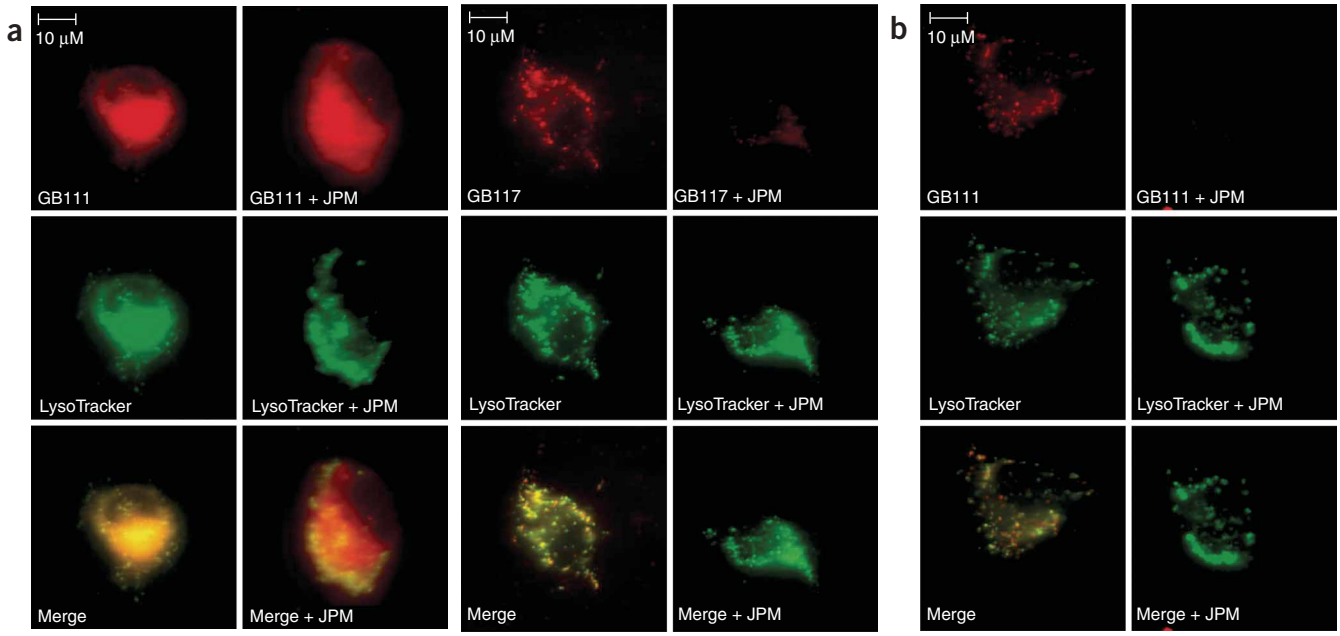

Figure 3 Imaging protease activity in live cells. (**a**) Cultures of NIH-3T3 cells were either pretreated with the general papain-family protease inhibitor JPM-OEt (50 μM) or with control DMSO (0.1%) for 1 h and labeled by addition of GB111 or GB117 (1 μM) to growth media for 4–5 h. The acidotropic lysosomal marker LysoTracker was added and cells were imaged with an inverted fluorescent microscope (Nikon). (**b**) Cells were treated and analyzed as in **a**, but were washed for 3 h in growth medium containing JPM-OEt (50 μM) or DMSO (0.1%) before imaging. Red fluorescence, protease activity; green fluorescence, lysosomal compartments; yellow color, overlap in green and red signals.

© 2005 Nature Publishing Group http://www.nature.com/naturechemicalbiology

was labeled efficiently by GB111 and only very poorly by GB117 and was absent in the cathepsin B–deficient cells. Furthermore, the two remaining species that were labeled by both probes were absent in the cathepsin L–knockout cells. These two bands represent the full-length single chain form and the cleaved heavy chain form of cathepsin L and are the two predominant active forms of cathepsin L observed in previous labeling studies[22]. Thus, the qABP and control probe freely penetrate cells and show highly specific labeling of cathepsins B and L in multiple cell lines.

On the basis of the positive biochemical results in the NIH-3T3 cells, we began fluorescent-imaging studies in these cells using both probes. Treatment of live monolayers of cells with GB111 followed by immediate imaging of the live cells with fluorescence microscopy showed intense, nonspecific staining of the entire cell, presumably as a result of free probe accumulation (**Fig. 3a**). The staining pattern for the unquenched control suggested that the probes do not accumulate in any particular location (that is, lipid bilayers) but rather distribute throughout the cell. Furthermore, the compounds showed no overall toxic effects on the cells even after overnight exposure. In contrast, when cells were incubated with GB117 and imaged without washing, a distinct punctate labeling pattern was observed. This pattern was found to overlap with the signal from the acidotropic lysosomal marker Lysotracker (Molecular Probes) and could be blocked by pretreatment of cells with the general inhibitor JPM-OEt. This pattern was highly consistent with specific labeling patterns that we had observed previously with fluorescent epoxide probes after extensive washing of the cells[15,27]. To confirm our analysis of the imaging data, we treated cells with GB111 and then performed extensive washing before microscopy-based imaging (**Fig. 3b**). As expected, the resulting images closely matched those observed for GB117. These results

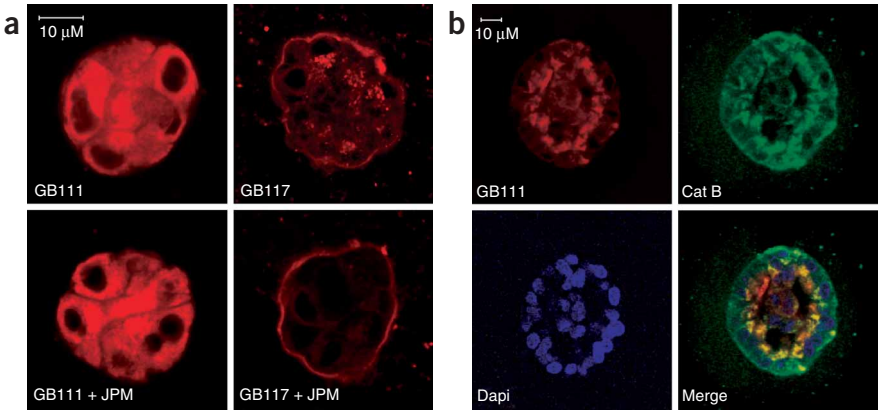

Figure 4 Imaging protease activity in three-dimensional cultured cells. (**a**) Reconstituted basement membrane, Cultrex (Trevigen) was mixed with GB111 or GB117 (1 μM) with or without JPM-OEt (50μM). MCF-10A cells were grown as three-dimensional cultures on Cultrex containing probes with or without inhibitor for three days then imaged by confocal microscopy with a water-immersion lens (Zeiss). (**b**) MCF-10A cells were grown on Cultrex without probes. Day 8 cultures were treated with GB111 (1 μM) for 3 h and then washed overnight with growth media. Cells were fixed and stained with antibodies recognizing human cathepsin B followed by incubation with a corresponding secondary antibody and DAPI. Cultures were imaged as in **a**.

© 2005 Nature Publishing Group http://www.nature.com/naturechemicalbiology

confirm that GB117 is fluorescently activated upon binding to protease targets and that this method provides sufficient signal over noise to allow direct real-time analysis of protease activity in live cells that have not been fixed or washed.

Finally, we wanted to apply the qABP to studies of more complex cell culture models. We chose to focus on a three-dimensional cell model that more accurately mimics human cancers[34]. The fibrocystic breast cell line MCF-10A forms highly organized three-dimensional spheroids when grown on reconstituted basement membranes (Cultrex). These structures recapitulate several aspects of glandular architecture *in vivo* and are therefore considered to be an excellent cellular model for various forms of tumor growth[35]. Because these cells presumably import and secrete components of the matrix, we reasoned that we should be able to apply the probes by direct addition to the matrix before seeding of cells. After three days of growth on matrix containing the probes, acinar structures had formed. Imaging of the samples grown on matrix containing the unquenched probe GB111 produced bright, nonspecific intracellular fluorescent staining similar to that observed in the monolayers (**Fig. 4a**). Interestingly, the free probe in the matrix did not show any significant fluorescence, suggesting a quenching effect by matrix proteins. Cells incubated on matrix containing the quenched probe GB117 showed distinct punctate staining of lysosomal compartments (**Fig. 4a**). Furthermore, this staining could be completely blocked by addition of the general inhibitor JPM-OEt, suggesting that it represents specific staining of active proteases. To confirm that the staining in the GB111-treated spheroids was due to background from free probe, we treated day 8 spheroids with GB111 and then washed and fixed the cells. Imaging of these spheroids showed specific staining similar to that observed in the live cells treated with GB117 (**Fig. 4b**). The resulting pattern of probe labeling partially overlapped with immunofluorescent staining of the same fixed cells with an anti-cathepsin B antibody. Interestingly, it appears that the population of active cathepsin B labeled by the probe is found predominantly at the apical pole of the cells in the acini, although the total distribution of cathepsin B protein is both apical and basal. These results further support the specific nature of the activity-based probes and also highlight the difference in imaging active protease populations rather than total protein levels with antibodies that recognize both precursor and active forms of protease.

In conclusion, we have developed a new class of qABPs that can be used to dynamically image protease activity in real time. The reagents described here target a very narrow subset of papain-family cysteine proteases. It should be possible to apply this methodology to a range of diverse cysteine proteases, as ABPs containing the AOMK warhead have recently been described that target multiple classes of cysteine proteases[9]. In addition, the use of this quenched-probe strategy can be easily adapted to incorporate near-infrared tags that may facilitate noninvasive, whole-body imaging applications. One of the main limitations to this strategy is the lack of signal amplification of the probes, thus potentially reducing their utility for whole-body methods. However, in some processes such as tumorigenesis, extensive local activation of proteases coupled with advances in the sensitivity of light-based imaging methods may allow direct imaging in live subjects with this approach. Such a step forward will also require probes with increased stability and bioavailability properties. We are currently working to develop the next generation of qABPs that will begin to address some of these important issues.

METHODS

General methods. Unless otherwise noted, all resins and reagents were purchased from commercial suppliers and used without further purification. All solvents used were HPLC grade. All water-sensitive reactions were performed in anhydrous solvents under positive pressure of argon. Reactions were analyzed by LC/MS with an API 150EX single quadrupole mass spectrometer (Applied Biosystems). Reverse-phase HPLC was conducted with an ÅKTA explorer 100 (Amersham Pharmacia Biotech) with C_{18} columns. High-resolution MS analyses were performed by the Stanford Proteomics and Integrative Research Facility with an Autoflex MALDI TOF/TOF mass spectrometer (Bruker). Fluorescent gels and plates were scanned with a Typhoon 9400 flatbed laser scanner (GE Healthcare).

Chemical synthesis and compound characterization. Please see the **Supplementary Methods** online section for details of the synthesis and characterization of probes.

Evaluation of *in vitro* quenching of the qABP. Dilutions of GB111 or GB117 in acetate buffer (50 mM acetate, 5 mM $MgCl_2$, 2 mM DTT, pH 5.5) containing 1% DMSO were prepared in a 96-well plate and measured with a Spectramax M5 fluorescence plate reader (Molecular Devices), with excitation (Ex) and emission (Em) at 535 and 574 nm, respectively. Relative fluorescent units (RFUs) were plotted versus probe concentration. The plate was then directly scanned with a Typhoon 9400 flatbed laser scanner (GE Healthcare), with Ex and Em at 532 and 580 nm, respectively.

Recombinant cathepsin labeling of the qABP. Recombinant human cathepsin L (0.7 μg; from V. Turk, Jozef Stefan Institute) or bovine cathepsin B (0.4 μg; Sigma) in reaction buffer (50 mM acetate, 2 mM DTT and 5 mM $MgCl_2$, pH 5.5) was treated with 25 μM JPM-OEt for 30 min (indicated samples) at 25 °C. Increasing concentrations of GB111 and GB117 were added to samples for 30 min. The reaction was stopped by addition of 4X sample buffer (40% glycerol, 0.2M Tris/HCl 6.8, 20% β-mercaptoethanol, 12% SDS and 0.4 mg ml^{-1} bromophenol blue). Half of the sample was separated on a 12% SDS gel and scanned by a Typhoon laser flatbed scanner at 532/580.

Determination of kinetic rate constants of inhibition. The kinetics of inhibition was determined by the progress curve method under pseudo-first-order conditions with at least ten-fold molar excess of inhibitor. Recorded progress curves were analyzed by nonlinear regression according to the following equation[36]:

$$[P] = v_z(1 - e^{-kt})/k$$

where [P] is the product, v_z is the velocity at time zero and k is the pseudo-first-order rate constant. Apparent rate constant (k_{app}) was determined from the slope of plot k versus [I]. Because of the irreversible and competitive mechanism of inhibition, k_{app} was converted to the association constant (k_{ass}) using the equation below:

$$k_{ass} = k_{app}(1+[S]/K_M)$$

Activity of human cathepsin L was measured with the fluorogenic substrate Z-FR-AMC[37] (Bachem; $K_m = 7.1$ μM) and cathepsin B was assayed against the fluorogenic substrate Z-RR-AMC[38] (Bachem; $K_m = 114$ μM). Concentration of substrates during the measurement was 10 μM. Cathepsins B and L (1 nM final concentrations) were incubated with inhibitor concentrations ranging from 10 to 2,000 nM in the presence of 10 μM of appropriate substrate. Total volume during the measurement was 100 μl. The increase in fluorescence (370-nm Ex, 460-nm Em) was continuously monitored for 30 min with a Spectramax M5 fluorescent plate reader (Molecular Devices), and inhibition curves were recorded. DMSO concentration during all measurements was 3.5%.

Cell cultures. NIH-3T3 mouse fibroblast cells (from P. Jackson, Stanford University) were cultured in DMEM supplemented with 10% FBS, 100 units ml^{-1} penicillin, 100 μg ml^{-1} streptomycin. WT mouse embryo fibroblasts (MEF) and *Cat* $L^{-/-}$ MEF cells (Roth *et al.*, 2000;) were from A. Nepveu (McGill University). *Cat* $B^{-/-}$ MEF cells were isolated and characterized in the laboratory of B.F.S. (L. Demchik and B.F.S., unpublished data). Cells were cultured in DMEM supplemented with 10% FBS, 100 units ml^{-1} penicillin, 100 μg ml^{-1} streptomycin. MCF-10A cells (from J. Brugge, Harvard University) were cultured in DMEM/F12 supplemented with 5% donor horse serum, 20 ng ml^{-1} EGF, 10 μg ml^{-1} bovine insulin, 0.5 μg ml^{-1}

hydrocortisone, and 1× antibiotic-antimycotic. All cells were cultured in a humidified atmosphere of 95% air and 5% CO_2 at 37 °C.

Labeling of intact cells with the control ABP and qABP. NIH 3T3 cells (250,000 cells per well) were seeded in a six-well plate one day before treatment. Cells were pretreated with the general papain-family protease inhibitor JPM-OEt (50 μM) or with control DMSO (0.1%) for 1 h and labeled by addition of GB111 and GB117 in DMSO at a given concentration to culture medium at pH 7.4 for indicated times. The final DMSO concentration was maintined at 0.2%. Cells were washed with PBS and lysed by addition of sample buffer (10% glycerol, 50 mM Tris/HCl, pH 6.8, 3% SDS, and 5% β-mercaptoethanol). Lysates were boiled for 10 min and cleared by centrifugation. Equal amounts of protein per lane were separated by 12% SDS-PAGE, and labeled proteases were visualized by scanning of the gel with a Typhoon flatbed laser scanner (Ex/Em 532/580 nm). WT, *Cat* $L^{-/-}$ and *Cat* $B^{-/-}$ MEF cells were labeled as described in the previous paragraph with few changes, with WT and *Cat* $L^{-/-}$ seeded at 240,000 cells per well and *Cat* $B^{-/-}$ seeded at 300,000 cells per well. GB111 or GB117 (1 μM) was added to the cells for 4.5 h before lysis.

Imaging protease activity in live cells. NIH 3T3 cells (165,000 cells per well) were seeded on glass coverslips in six-well tissue culture plates containing growth medium one day before treatment. Cells were either pretreated with the general papain-family protease inhibitor JPM-OEt (50 μM) or with control DMSO (0.1%) for 1 h. Cells were labeled by addition of GB111 or GB117 (1 μM) to growth media at pH 7.4 for 4–5 hours. Cells were transferred to growth medium without phenol red. LysoTracker (50 nM final concentration) was added minutes before cells were imaged with an inverted fluorescent microscope (Nikon Diaphot-300 microscope with a 60X (NA 1.4) objective). Cells were washed with growth medium containing JPM-OEt (50 μM) or with control DMSO (0.1%) for 3 h and imaged.

Imaging protease activity in three-dimensional cultured cells. MCF-10A cells were grown in three-dimensional culture on reconstituted basement membrane extracted from an EHS mouse sarcoma (Cultrex from Trevigen) as previously described[35]. GB117 or GB111 was added to Cultrex (1 μM final concentration) upon cell seeding, and day 3 structures were imaged as described in the next paragraph. Day 8 structures grown in Cultrex without probes were treated with 1 μM GB111 for 3 h in assay medium (culture medium with 2% horse serum and 5 ng ml^{-1} EGF). Cells were washed overnight in assay medium, fixed and imaged as described below.

Immunofluorescence analysis. Cells in three-dimensional culture were fixed on day 8 with cold methanol for 10 min and washed with PBS three times at 10 min per wash. Structures were then blocked for 1 h in IF buffer (130 mM NaCl, 7mM Na_2HPO_4, 3.5 mM NaH_2PO_4, 7.7 mM NaN_3, 0.1% bovine serum albumin, 0.2% triton X-100, 0.05% TWEEN 20) and incubated with a rabbit anti-human cathepsin B (produced and characterized in the laboratory of B.F.S.[39]) antibody overnight at 4 °C. Structures were washed three times with PBS for 20 min per wash and then incubated with the corresponding secondary antibody for 2 h at room temperature, and then washed three times with PBS for 20 min each time. Structures were incubated with 1 μg ml^{-1} DAPI in PBS for 10 min and then washed three times with PBS. Samples were imaged with a 40× water immersion lens on a Zeiss LSM 510 confocal microscope.

Computer modeling of GB111 and GB117 structures of cathepsins B and L. GB111 and GB117 were docked into cathepsin B (1SP4) and cathepsin L (1MHW) with the MMF94 force field using molecular operating environment (Chemical Computing Group). During the simulation, the backbone of both the protein and ligand were constrained, whereas the side chains were allowed full relaxation. Pictures were rendered with Pymol (Delano Scientific LLC, http://pymol.sourceforge.net).

Note: Supplementary information is available on the Nature Chemical Biology website.

ACKNOWLEDGMENTS

We thank B. Goulet and A. Nepveu (McGill University) for cathepsin L–deficient MEF cells and V. Turk and B. Turk (J. Stefan Institute) for recombinant human cathepsin L. The authors thank C. Gilon for helpful advice on peptide synthesis, G. von Degenfeld for technical assistance throughout the project, K. Boatright and S. Verhelst for helpful discussion of the manuscript. This work was supported by a Turman Fellowship at Stanford University (to M.B.), a US National Institutes of Health National Technology Center for Networks and Pathways grant U54 RR020843 (to M.B.), and a Department of Defense Breast Cancer Center of Excellence grant DAMD-17-02-0693 (to B.F.S.; M.B. subcontract).

COMPETING INTERESTS STATEMENT

The authors declare that they have no competing financial interests.

Received 20 June; accepted 20 July 2005
Published online at http://www.nature.com/naturechemicalbiology/

1. Puente, X.S., Sánchez, L.M., Overall, C.M. & López-Otín, C. Human and mouse proteases: a comparative genomic approach. *Nat. Rev. Genet.* **4**, 544–558 (2003).
2. Baruch, A., Jeffery, D.A. & Bogyo, M. Enzyme activity–it's all about image. *Trends Cell Biol.* **14**, 29–35 (2004).
3. Berger, A.B., Vitorino, P.M. & Bogyo, M. Activity-based protein profiling: applications to biomarker discovery, in vivo imaging and drug discovery. *Am. J. Pharmacogenomics* **4**, 371–381 (2004).
4. Speers, A.E. & Cravatt, B.F. Chemical strategies for activity-based proteomics. *ChemBioChem* **5**, 41–47 (2004).
5. Jeffery, D.A. & Bogyo, M. Chemical proteomics and its application to drug discovery. *Curr. Opin. Biotechnol.* **14**, 87–95 (2003).
6. Adam, G.C., Sorensen, E.J. & Cravatt, B.F. Chemical strategies for functional proteomics. *Mol. Cell. Proteomics* **1**, 781–790 (2002).
7. Jessani, N. & Cravatt, B.F. The development and application of methods for activity-based protein profiling. *Curr. Opin. Chem. Biol.* **8**, 54–59 (2004).
8. Liu, Y., Patricelli, M.P. & Cravatt, B.F. Activity-based protein profiling: the serine hydrolases. *Proc. Natl. Acad. Sci. USA* **96**, 14694–14699 (1999).
9. Kato, D. *et al.* Activity-based probes that target diverse cysteine protease families. *Nat. Chem. Biol.* **1**, 33–38 (2005).
10. Bogyo, M., Shin, S., McMaster, J.S. & Ploegh, H.L. Substrate binding and sequence preference of the proteasome revealed by active-site-directed affinity probes. *Chem. Biol.* **5**, 307–320 (1998).
11. Bogyo, M., Verhelst, S., Bellingard-Dubouchaud, V., Toba, S. & Greenbaum, D. Selective targeting of lysosomal cysteine proteases with radiolabeled electrophilic substrate analogs. *Chem. Biol.* **7**, 27–38 (2000).
12. Saghatelian, A., Jessani, N., Joseph, A., Humphrey, M. & Cravatt, B.F. Activity-based probes for the proteomic profiling of metalloproteases. *Proc. Natl. Acad. Sci. USA* **101**, 10000–10005 (2004).
13. Chan, E.W., Chattopadhaya, S., Panicker, R.C., Huang, X. & Yao, S.Q. Developing photoactive affinity probes for proteomic profiling: hydroxamate-based probes for metalloproteases. *J. Am. Chem. Soc.* **126**, 14435–14446 (2004).
14. Greenbaum, D., Medzihradszky, K.F., Burlingame, A. & Bogyo, M. Epoxide electrophiles as activity-dependent cysteine protease profiling and discovery tools. *Chem. Biol.* **7**, 569–581 (2000).
15. Greenbaum, D. *et al.* Chemical approaches for functionally probing the proteome. *Mol. Cell. Proteomics* **1**, 60–68 (2002).
16. Falgueyret, J.P. *et al.* An activity-based probe for the determination of cysteine cathepsin protease activities in whole cells. *Anal. Biochem.* **335**, 218–227 (2004).
17. Hemelaar, J. *et al.* Specific and covalent targeting of conjugating and deconjugating enzymes of ubiquitin-like proteins. *Mol. Cell. Biol.* **24**, 84–95 (2004).
18. Borodovsky, A. *et al.* A novel active site-directed probe specific for deubiquitylating enzymes reveals proteasome association of USP14. *EMBO J.* **20**, 5187–5196 (2001).
19. Borodovsky, A. *et al.* Small-molecule inhibitors and probes for ubiquitin- and ubiquitin-like-specific proteases. *ChemBioChem* **6**, 287–291 (2005).
20. Greenbaum, D.C. *et al.* A role for the protease falcipain 1 in host cell invasion by the human malaria parasite. *Science* **298**, 2002–2006 (2002).
21. Yasothornsrikul, S. *et al.* Cathepsin L in secretory vesicles functions as a prohormone-processing enzyme for production of the enkephalin peptide neurotransmitter. *Proc. Natl. Acad. Sci. USA* **100**, 9590–9595 (2003).
22. Goulet, B. *et al.* A cathepsin L isoform that is devoid of a signal peptide localizes to the nucleus in S phase and processes the CDP/Cux transcription factor. *Mol. Cell* **14**, 207–219 (2004).
23. Baruch, A. *et al.* Defining a link between gap junction communication, proteolysis, and cataract formation. *J. Biol. Chem.* **276**, 28999–29006 (2001).
24. Mahrus, S. & Craik, C.S. Selective chemical functional probes of granzymes A and B reveal granzyme B is a major effector of natural killer cell-mediated lysis of target cells. *Chem. Biol.* **12**, 567–577 (2005).
25. Jessani, N., Liu, Y., Humphrey, M. & Cravatt, B.F. Enzyme activity profiles of the secreted and membrane proteome that depict cancer cell invasiveness. *Proc. Natl. Acad. Sci. USA* **99**, 10335–10340 (2002).
26. Jessani, N. *et al.* Carcinoma and stromal enzyme activity profiles associated with breast tumor growth in vivo. *Proc. Natl. Acad. Sci. USA* **101**, 13756–13761 (2004).
27. Joyce, J.A. *et al.* Cathepsin cysteine proteases are effectors of invasive growth and angiogenesis during multistage tumorigenesis. *Cancer Cell* **5**, 443–453 (2004).
28. Okerberg, E.S. *et al.* High-resolution functional proteomics by active-site peptide profiling. *Proc. Natl. Acad. Sci. USA* **102**, 4996–5001 (2005).

© 2005 Nature Publishing Group http://www.nature.com/naturechemicalbiology

29. Powers, J.C., Asgian, J.L., Ekici, O.D. & James, K.E. Irreversible inhibitors of serine, cysteine, and threonine proteases. *Chem. Rev.* **102**, 4639–4750 (2002).
30. Sando, S. & Kool, E.T. Quencher as leaving group: efficient detection of DNA-joining reactions. *J. Am. Chem. Soc.* **124**, 2096–2097 (2002).
31. Sando, S. & Kool, E.T. Imaging of RNA in bacteria with self-ligating quenched probes. *J. Am. Chem. Soc.* **124**, 9686–9687 (2002).
32. Turk, D., Guncar, G., Podobnik, M. & Turk, B. Revised definition of substrate binding sites of papain-like cysteine proteases. *Biol. Chem.* **379**, 137–147 (1998).
33. Musil, D. *et al.* The refined 2.15 A X-ray crystal structure of human liver cathepsin B: the structural basis for its specificity. *EMBO J.* **10**, 2321–2330 (1991).
34. O'Brien, L.E., Zegers, M.M. & Mostov, K.E. Opinion: Building epithelial architecture: insights from three-dimensional culture models. *Nat. Rev. Mol. Cell Biol.* **3**, 531–537 (2002).
35. Debnath, J., Muthuswamy, S.K. & Brugge, J.S. Morphogenesis and oncogenesis of MCF-10A mammary epithelial acini grown in three-dimensional basement membrane cultures. *Methods* **30**, 256–268 (2003).
36. Bieth, J.G. Theoretical and practical aspects of proteinase inhibition kinetics. *Methods Enzymol.* **248**, 59–84 (1995).
37. Barlic-Maganja, D., Dolinar, M. & Turk, V. The influence of Ala205 on the specificity of cathepsin L produced by dextran sulfate assisted activation of the recombinant proenzyme. *Biol. Chem.* **379**, 1449–1452 (1998).
38. Deval, C., Bechet, D., Obled, A. & Ferrara, M. Purification and properties of different isoforms of bovine cathepsin B. *Biochem. Cell Biol.* **68**, 822–826 (1990).
39. Moin, K. *et al.* Human tumour cathepsin B. Comparison with normal liver cathepsin B. *Biochem. J.* **285**, 427–434 (1992).

© 2005 Nature Publishing Group http://www.nature.com/naturechemicalbiology